Application range of the HEM approach for CO_2 expansion inside two-phase ejectors for supermarket refrigeration systems

Michal Palacz[a,*], Jacek Smolka[a], Adam Fic[a], Zbigniew Bulinski[a], Andrzej J. Nowak[a], Krzysztof Banasiak[b], Armin Hafner[b]

[a] *Institute of Thermal Technology, Silesian University of Technology, Konarskiego 22, 44-100 Gliwice, Poland*
[b] *SINTEF Energy, Kolbjørn Hejes v. 1D, Trondheim, 7465, Norway*

Abstract

In this study, the accuracy of the homogeneous equilibrium (HEM) applied to 3-D CFD-based simulations of CO_2 expansion inside two-phase ejectors is presented. The HEM approach previously reported in the literature were assessed by comparing the computed and measured mass flow rates that pass through an ejector motive nozzle. In addition, the HEM approach implemented using CFD was tested over a vast range of ejector operating regimes. To ensure that all of the computations were performed consistently, a validated CFD model combined within an in-house developed script was used. The comparison of the experimental and computational results showed that the HEM accuracy varied for the different sets of operating parameters. Accurate results were obtained for operating regimes near or above the CO_2 critical point. The model accuracy decreased with the decreasing temperature and decreasing distance to the saturation line.

Keywords: HEM, R744, ejector, two-phase CO_2, ejector efficiency

Nomenclature

c_p	specific heat, kJ kg^{-1} K^{-1}
E	total enthalpy, kJ kg^{-1}
h	specific enthalpy, kJ kg^{-1}
k	effective thermal conductivity, W m^{-1}K^{-1}
$\dot{m}$	mass flow rate, kg s^{-1}
p	pressure, Pa
s	specific entropy, kJ kg^{-1} K^{-1}
T	temperature, K
t	time, s
$\boldsymbol{U}$	velocity vector, m s^{-1}
x	actual vapour quality, –

Greek Symbols

*Tel.: +48 322372810; fax: +48 322372872
michal.palacz@polsl.pl

χ mass entrainment ratio, -

δ relative difference, %

η overall ejector efficiency, %

μ dynamic viscosity, kJ kg^{-1}

ρ density, kg m^{-1}

τ stress tensor, N m^{-2}

θ relaxation time, s

Subscripts

CFD computed value

dif diffuser

EJ ejector

eq equilibrium

EXP measured value

i number

in inlet

l liquid phase

mn motive nozzle

out outlet

s saturation

sn suction nozzle

v vapour phase

1. Introduction

Due to high global warming potential (GWP) of currently used synthetic refrigerants, the natural refrigerant carbon dioxide (R744) is a promising alternative. The GWP of CO_2 is 1 by definition, whereas the GWP of the popular refrigerant R143a is 4300. Additionally, R744 is classified as a non-toxic and non-flammable fluid. A drawback regarding the use of the carbon dioxide in refrigeration systems is the relatively low efficiency of the corresponding units, especially at high ambient temperatures. Under such conditions, the throttling losses are significant when standard expansion valve is used. To partially recover these losses, ejectors have been introduced to the systems (Elbel (2011)).

The experimental study by Elbel and Hrnjak (2008) compared the coefficient of performance (COP) of the conventional R744 refrigeration system with the expansion valve to a system equipped with an ejector that was installed to reduce the throttling losses of the expansion valve. Moreover, the authors introduced the dimensionless factor, termed the overall ejector efficiency (η_{EJ}) to assess the ejector performance. The results of this investigation showed that the COP of the ejector system increased by 7%, suggesting that the ejector-based systems can be an alternative to expansion valve systems.

To better understand the ejector performance, many numerical and experimental studies have been carried out. Nakagawa et al. (2011) investigated the effect of the mixing length on the performance of two-phase ejectors. The authors reported that an improper mixer length yielded a decrease in the COP by as much as 10%.

Liu et al. (2012) analysed an effect of various parameters of the investigated ejector, such as the ambient temperature, the compressor frequency and the motive nozzle throat diameter, on refrigeration system performance. A decrease in the throat diameter increased the COP by up to 60%. The influence of the geometrical mixer and the diffuser configuration of the ejector on the system COP were also experimentally and numerically investigated by Banasiak et al. (2012).

The discussed literature suggests that the ejector geometry significantly affects the overall ejector performance and, consequently, the COP of the refrigeration unit. Therefore, a variety of mathematical approaches have been developed, including relatively simple 1-D models and more complex 2-D and 3-D CFD formulations.

Liu and Groll (2008) used a 1-D model to design a basic ejector shape. In this approach, the isentropic efficiency of each section was assumed. Then, the dimensions of all of the parts were defined. The general model was divided in to submodels, and each model represented different parts of the ejector structure, such as the motive nozzle, the suction nozzle, the mixer and the diffuser. For all of these submodels and ejector parts, except the diffuser, the specific efficiencies were assumed and then adjusted to compensate for the differences between the computed and measured mass flow rates. The proposed flow model was based on the approach introduced by Katto (1969), where the two-phase critical flow was treated as a homogeneous equilibrium two-phase flow.

A more complex 1-D model was developed by Banasiak and Hafner (2011). Similar to the work of Liu and Groll (2008), the model was divided into submodels, but the domain division was different. Those submodels were related to the flow characteristics of each section. Hence, in this approach, the submodels consisted of a single-flow model for the motive and suction nozzle and a pre-mixing chamber model and a two-flow model for the mixer and the diffuser. For each submodel, a set of the governing equations was introduced. The fluid flow for the single-flow was assumed to be homogeneous. In addition, the thermodynamic state of the fluid was modelled using a delayed equilibrium model (DEM) (Attou and Seynhaeve (1999)) that was enhanced according to the homogeneous nucleation theory (HNT) (Kolev (2005)) to analyse the metastable effects inside the motive nozzle. The refrigerant flow in the two-flow passages was modelled using the HEM approach. The model was validated against the measured pressure lifts and the critical mass flow rates. The discrepancies were satisfactory low, i.e., the average pressure lift was only 2.7%.

For more accurate computations within 3-D ejector geometries, Smolka et al. (2013) formulated a mathematical model based on the homogeneous real fluid approach to simulate carbon dioxide flow inside transonic ejectors. The authors used a commercial Ansys Fluent solver with developed user defined functions (UDFs) to substitute the standard temperature-based energy equation with the enthalpy-based form and to define real fluid properties based on the REFPROP libraries (Lemmon et al. (2010)). Moreover, 3-D computational domains were considered to show the influence of the side inlet arrangement. The validation procedure was based on comparing the mass flow rates obtained using the CFD with those obtained experimentally, revealing differences below 15%.

Similarly, Lucas et al. (2014)investigated CO_2 ejectors numerically. As in the work of Smolka et al. (2013), thermodynamic and mechanical equilibria were assumed for the two-phase flow. In that study, an energy equation was formulated in the same manner as in the model described previously. However, in the Lucas et al. (2014) study, OpenFOAM solver was used instead of commercial software. The TEMO-media library was used to obtain the physical properties of the real fluid. This model was also validated against experimentally determined mass flow rates. The differences between the computed and measured motive nozzle mass flow rate were below 10%. However, the differences in the predicted pressure recovery without and with suction flow for simulation of the ejector were below 10% and 20%, respectively.

To describe the physics of the supercritical fluid flow with better fidelity, Yazdani et al. (2012) used a nonhomogeneous mixture model. The model utilised the additional set of equations to simulate the phase change caused by cavitation and boiling. In Yazdani et al. (2012), ejectors were investigated both numerically and experimentally. The additional equations were implemented using the Ansys Fluent solver. For turbulence modelling, the SST $K-\omega$ model was applied. . The real fluid properties were obtained by implementing the REFPROP libraries (Lemmon et al. (2010)) for the supercritical fluid, the subcooled liquid and the inside the saturation region and the Peng-Robinson equation of state for the superheated vapour. The numerical results in the form of pressure profiles agreed well with the measured data. Furthermore, the difference between the simulated and measured mass entrainment ratios (MER) was below 10%.

Colarossi et al. (2012)proposed a homogeneous relaxation model (HRM) to simulate CO_2 with a higher accuracy. OpenFOAM solver and the REFPROP libraries were used to perform all of the computations. Similar to Lucas et al. (2014), the computational domain was axisymmetric, and the $K-\epsilon$ model was used to simulate the turbulence. The authors of that investigation compared the instantaneous quality of the fluid with the equilibrium quality. The observed differences were negligible, especially inside the diffuser. The numerical results were compared to the experimental data reported by Nakagawa et al. (2011) in terms of the pressure recovery. In some cases, the reported differences were relatively high, although similar trends were observed.

According to the studies reviewed here, both models (HEM and HRM) agree well with experimental results. Nevertheless, Benintendi (2014) reported that under some operating conditions, the HEM accuracy is not satisfactory. Therefore, the quality of the HEM should be assessed over wider range of operating regimes, especially regarding the accuracy of the model for the typical operating regimes typical of refrigeration systems. Hence, the objective of this study was to define the range of the motive nozzle operating conditions for which the HEM approach provides reasonable results. To evaluate the HEM accuracy, the computed motive nozzle mass flow rate was compared to the measured motive nozzle mass flow rate. To the best of our knowledge, such a systematic and vast investigation of HEM performance for the converging-diverging nozzles has not yet been published.

2. Modelling approach and computational procedure

2.1. HEM model

One of the most common approaches used to model the two-phase flow of CO_2 is based on the implementation of HEM and HRM models (Smolka et al. (2013), Lucas et al. (2014), Colarossi et al. (2012)). The HEM was employed to perform all of the computations.

The mass, momentum and energy equations for that approache are described by the following set of equations:

$$\frac{\partial \rho}{\partial t} + \nabla \cdot (\rho \boldsymbol{U}) = 0 \tag{1}$$

$$\frac{\partial (\rho \boldsymbol{U})}{\partial t} + \nabla \cdot (\rho \boldsymbol{U}\boldsymbol{U}) = -\nabla p + \nabla \cdot \tau \tag{2}$$

$$\frac{\partial (\rho E)}{\partial t} + \nabla \cdot (\rho \boldsymbol{U} E) = \frac{\partial p}{\partial t} + \nabla \cdot (k \nabla T + \tau \cdot \boldsymbol{U}) \tag{3}$$

The total enthalpy is defined as the sum of the mixture specific enthalpy and the kinetic energy.

$$E = h + \frac{U^2}{2} \tag{4}$$

The homogeneous equilibrium model is based on the assumption that the local quantities of velocity, pressure and temperature are the same for the liquid and the gaseous phases. Hence, the mechanical and thermodynamic equilibria of both phases are assumed as:

$$\begin{cases} p_l = p_v = p \\ T_l = T_v = T \\ U_l = U_v = U \end{cases} \tag{5}$$

As a consequence, all of the fluid properties are a function of pressure and enthalpy:

$$\left\{\rho, \mu, k, c_p\right\} = f(p, h) \tag{6}$$

For the steady state computations, all of the time derivatives in Eqs. (1)-(3) were neglected.

2.2. Computational procedure

The mathematical model used to perform all of the computations in this study was based on the HEM and implemented using the commercial Ansys Fluent platform (Smolka et al. (2013)). A set of boundary conditions was defined for the ejector inlets and outlet to complete the mathematical description of the fluid flow. The pressure and the temperature were considered as the input data for both of the ejector inlets and the unit outlet. The values of the inlets and outlet pressures were measured at the SINTEF Energy laboratory during the experimental investigation of the ejectors. The liquid phase was considered as the primary stream, and the vapour CO_2 was sucked through the suction nozzle. The typical range of the inlets and outlet parameters was considered for an ejector operating in a supermarket refrigeration unit Hafner et al. (2014). All the considered inlet parameters of the motive and suction nozzles as well as the ejector outlet pressure are presented in Tab. 2. In addition, experimentally determined efficiency for each considered operating regimes is presented in that table. The ejector efficiency was defined as in Eq. (8). The discussion of the measured values and a comparison of the numerical results are given in Section 3.4.

The 3-D ejector geometry was considered as the computational domain and was discretised to fully structure the grid. To eliminate the influence of discretisation, extensive computations were carried out for a number of mesh sizes. As a result of the mesh sensitivity study, a grid consisting of approximately 140 thousand hexahedral elements was selected. The mesh was refined in regions where sonic waves usually occur.

The above model definitions were coded in text scripts of commercial Ansys packages, such as Ansys ICEM and Ansys Fluent, to automatically run all of the computations in a repeating manner. The scheme of the code is presented in Fig. 1. The geometry description and the mesh parameters were stored in an external input file. However, the global mesh parameters were constant for all of the cases. Then, the geometry and the mesh input file were loaded to the preprocessor, where geometrical model was generated and discretised. Next, the control script executed the computations by first loading the generated mesh into the solver and then setting up the model using the input values of the boundary conditions. The PRESTO scheme was used for pressure discretisation. All of the remaining variables were discretised using a second-order upwind scheme. The coupled method was employed for the velocity and pressure coupling. As it was mentioned in the Section 1, the real fluid properties were obtained by the implementation the REFPROP libraries Lemmon et al. (2010) in to the Ansys Fluent solver.

To model the turbulence, the realisable $K-\epsilon$ model was employed in this investigation. This approach has been tested by a number of authors, including Smolka et al. (2013),Varga et al. (2009), or Rusly et al. (2005) who have reported satisfactory results. The exact form of the transport equations of the turbulent kinetic energy K and the kinetic energy dissipation rate ϵ have been widely described in the literature (Chung (2010)).

When the solution was converged, post-processing was executed using the control script. As a result, the numerical values describing the ejector performance and all of the parameters of the operation diagnostics were exported to a result text file. In addition, the contours of the flow variables were saved to graphics files. The entire computational time was approximately 20 hours for the test case using 10-node parallel processes.

3. Parameter range vs. HEM accuracy

3.1. Measurements

All of the measured values were captured in the SINTEF Energy laboratory during the investigation of the multi-ejector refrigeration unit for supermarkets. That refrigeration systems was rated for 70 kW at a 35°C gas cooler outlet temperature and -3°C evaporation temperature. The multi-ejector unit installed in the refrigeration system was equipped in four ejectors (EJ1-EJ4) which were designed for different cooling capacity of the system. Thus, the motive nozzle were designed for different system loads. The dimensions of these motive nozzles are presented in Tab. 1. The more detailed information about the refrigeration unit are presented in the paper of Banasiak et al. (2015).

The mentioned test rig was equipped with PT1000 calibrated thermocouples, calibrated piezoelectric elements for the pressure measurements and calibrated Coliris type mass flow metres. The accuracy of these elements was as follows: $\pm$ 0.6 K for temperature measurements, $\pm$ 2.5×10^{4} Pa for the pressure measurements, and $\pm$ 0.5×10^{-3} kg·s^{-1} for the mass flow rate measurements. All of the sensors were connected to a Danfoss controller interfaced with Danfoss Minilog software to monitor the measured data.

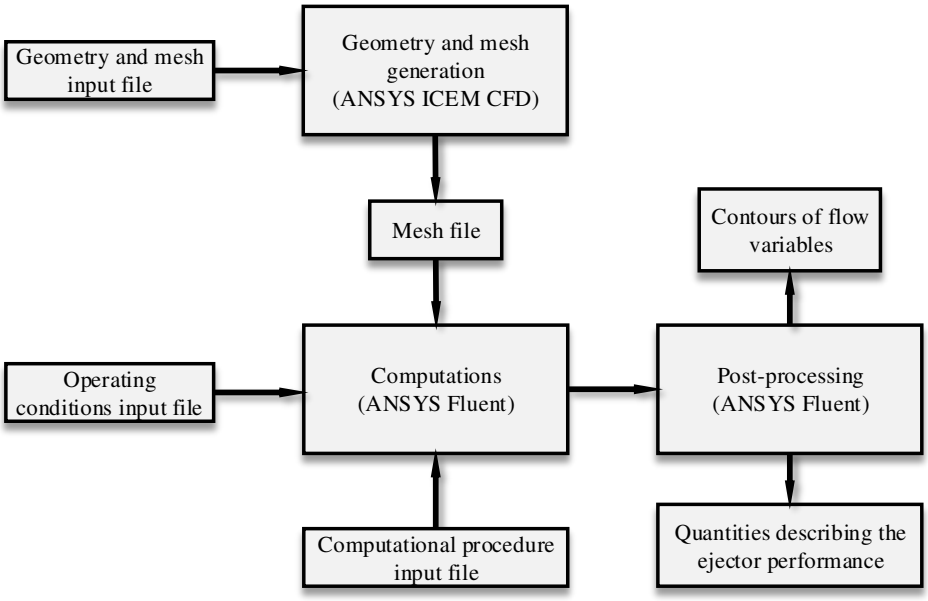

Figure 1: Scheme of the control script structure for the automatic computations.

Table 1: The geometrical parameters of the ejector motive nozzles of the multi-ejector unit (Banasiak et al. (2015))

	EJ1	EJ2	EJ3	EJ4
Motive nozzle inlet diameter, 10^{-3} m	3.80	3.80	3.80	3.80
Motive nozzle throat diameter, 10^{-3} m	1.00	1.41	2.00	2.83
Motive nozzle outlet diameter, 10^{-3} m	1.12	1.58	2.24	3.16
Motive nozzle diverging angle, °	2.00	2.00	2.00	2.00
Motive nozzle converging angle, °	30.00	30.00	30.00	30.00

3.2. Definitions

The results obtained using the computational tool described in Section 2.2 were compared with the measured data to assess the accuracy of the approach under various operating conditions. Comparisons were performed similarly to previous reports (Lucas et al. (2014), Colarossi et al. (2012), Yazdani et al. (2012) Smolka et al. (2013)).In such previous studies, to evaluate the model accuracy, the measured and the predicted mass flow rates were compared. The ejector performance parameter, termed the mass entrainment ratio (χ) was compared with the experimental data. χ is the ratio between the secondary and the primary mass flow rates of the ejector:

$$\chi = \frac{\dot{m}_{sn}}{\dot{m}_{mn}} \tag{7}$$

This parameter is very important because it significantly affects the overall ejector efficiency, which was defined by Elbel (2011) in the following form:

$$\eta = \chi \cdot \frac{h\big|_{s=s_{sn,in}\ p=p_{dif,out}} - h_{sn,in}}{h_{mn,in} - h\big|_{s=s_{mn,in}\ p=p_{dif,out}}} \tag{8}$$

Considering the relation of χ and η, under or overestimated mass flow rates can result from a poorly estimated overall ejector efficiency. In the cited papers, to express the discrepancy between the measured and simulated values, the

relative difference was used in the following form:

$$\delta_i = \left(1 - \frac{i_{EXP}}{i_{CFD}}\right) \cdot 100 \tag{9}$$

3.3. Previous applications of the HEM/HRM approach

The authors of this paper focused on the accuracy of the simulation of the primary flow expansion inside the motive nozzle. Hence, the comparison of the motive nozzle mass flow rate was the most important parameter defining the model accuracy. In addition, the analysis of the measured and computed mass entrainment ratio was performed to assess the influence of the primary mass flow rate on the secondary mass flow rate.

Yazdani et al. (2012) showed good agreement between experimental and simulation results. The difference between the measured and computed data was less than 10% in almost all of the computed cases. However, Yazdani et al. (2012) provides only the full information regarding the baseline boundary conditions for the ejector. The motive nozzle inlet pressure and temperature were set to 123.3 bar and 40°C, respectively. Unfortunately, no information is provided regarding the other investigated points. Nevertheless, the errors of the motive nozzle mass flow rates and were relatively small. Only for one computed case was the error of the motive nozzle mass flow rate slightly higher than 10%. Moreover, the analysed pressure profiles agreed well between the computational and experimental results. However, a lack of the information regarding the remaining considered motive nozzle inlet parameters made it difficult to assess the general accuracy of the reported approach.

The classical HRM was also used by Colarossi et al. (2012). The numerical results were compared with the experimental results presented by Nakagawa et al. (2011). However, Colarossi et al. (2012) compared the measured and computed pressure recoveries, defined as the difference between the ejector outlet pressure and the suction inlet pressure. The comparison revealed the errors up to nearly 50%. Unfortunately, the authors used fixed mass flow rates at the boundaries, and hence the assessment of the accuracy of the HRM approach based on the comparison of the computed and experimental determined mass flow rates was impossible.

Lucas et al. (2014) performed an extensive numerical investigation of ejector performance parameters. The authors described the considered inlet parameters in detail. The presented numerical results exhibited high agreement with the experimentally captured data, especially when the ejector operated as a throttling nozzle, i.e., the suction nozzle was closed. Under such conditions, the relative differences were between -5% and +5% for the motive nozzle mass flow rates. Although a vast number of points were investigated, the range of the operating parameters was rather narrow. All of the motive nozzle inlet parameters were distributed close or above the R744 critical point.The distribution of parameters used by Lucas et al. (2014) is presented in Fig. 2. The critical point for carbon dioxide is denoted with a pink asterisk, and the red circles denote the investigated inlet parameters to the motive nozzle. Most of the test cases were computed for temperatures of 30°C, 35°C and 40°C. The pressure ranged from 72.6 bars to 102.7 bars. However, the pressure changes for the specific temperature were not significant. Nonetheless, the analysed parameter range was relatively small, and the results showed that use of the HEM under such conditions was a highly effective and accurate approach.

3.4. HEM accuracy for sub- and supercritical parameters

To better assess the accuracy of the HEM approach, extensive numerical simulations were performed in this study. The range of considered inlet parameters was typical for ejectors operating in refrigeration installations of supermarkets (Hafner et al. (2014), Banasiak et al. (2015)).

For some cases, the investigated parameters are similar to those reported by Lucas et al. (2014), e.g., points #2 and #3. However, the operating motive nozzle inlet pressure was maintained at the same level to investigate the influence of decreasing temperature on the model accuracy (see points #2, #5 and #13 in Tab. 2. Moreover, other points were placed far left from the critical point. Hence, the temperature at these points was significantly lower than that of the critical point. Point #18 denotes the operating regime of the lowest temperature.

The points distributed close to the critical points guarantee accurate results. For points #1, #2, #4 and #6, the motive nozzle mass flow rate error was approximately 5%. For such operating regimes, the results obtained here are within the same accuracy as those reported in the literature (Yazdani et al. (2012); Lucas et al. (2014)). Furthermore,

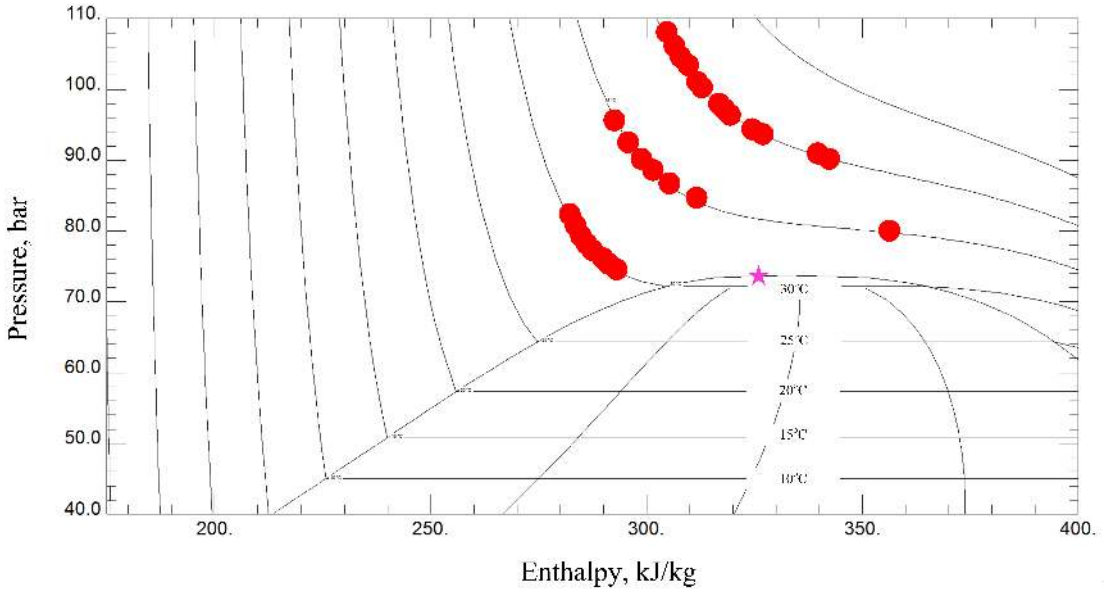

Figure 2: Distribution of the motive nozzle inlet parameters numerically investigated in the paper of Lucas et al. (2014).

the mass flow rates for the points that are described with the inlet pressure higher than the critical pressure are also predicted well. However, this accuracy decreases with the decreasing temperature. For example, the pressure difference between points #7 and #17 is relatively small, approximately 3 bars, whereas the temperature and the resulting motive nozzle mass flow rate differences are significant. However, the model is inaccurate in some areas near the saturation line, which can be observed when comparing the errors for points #16 and #18 or #11 and #12.

In addition to the description of the analysed operating regimes, the relative differences in the motive and the suction nozzle mass flow rates and the resulting χ are listed in this table. We also assessed whether χ compensated for the prediction error between the primary and secondary mass flow rates. The results showed that, in most cases, the unpredicted motive nozzle mass flow rate results in the χ errors. However, in specific cases, the unpredicted motive nozzle mass flow rate does not affect the χ prediction accuracy, e.g. point #18. For this case, the χ error is strongly related to the motive nozzle mass flow rate error. Nevertheless, the underestimated latter parameter results in an overestimated mass entrainment ratio. Hence, a comparison of the measured and computed χ should not be used to assess the HEM/HRM accuracy. Moreover, an improperly determined χ can significantly influence the overall ejector efficiency (Eq. (8)), which is unacceptable for the optimisation of the ejector geometry that may be performed using the HEM approach.

Table 2: Comparison of the computed results with the experimental data.

No.	Motive nozzle		Suction nozzle		Outlet	Exp.		CFD		δ_m,%	δ_s,%	δ_χ, %	η_{EXP}, %
	p_{in}, bar	T_{in}, °C	p_{in}, bar	T_{in}, °C	p_{out}	$\dot{m}_m$, kg/s	$\dot{m}_s$, kg/s	$\dot{m}_m$, kg/s	$\dot{m}_s$, kg/s				
1	91.14	35.19	28.25	4.53	39.30	0.157	0.029	0.169	0.035	7.10	17.14	10.81	24.00
2	76.67	28.25	28.04	16.40	32.89	0.143	0.055	0.133	0.055	-7.52	0.00	0.00	31.00
3	95.90	36.39	28.97	21.65	37.92	0.170	0.052	0.185	0.052	8.11	0.00	-8.82	31.00
4	85.61	33.06	29.00	17.32	34.96	0.144	0.060	0.144	0.061	0.00	1.64	1.64	33.00
5	74.71	27.79	28.77	15.91	34.06	0.132	0.050	0.138	0.051	4.35	1.96	-2.50	34.00
6	85.31	29.65	28.11	18.67	33.43	0.175	0.059	0.166	0.056	-5.42	-5.36	0.06	27.00
7	68.85	25.10	28.41	14.09	34.23	0.128	0.035	0.124	0.035	-3.23	0.00	3.13	32.00
8	66.56	24.17	28.82	14.00	36.71	0.128	0.009	0.113	0.006	-13.27	-50.00	-32.42	12.00
9	64.03	21.91	28.43	14.72	36.59	0.144	0.006	0.122	0.000	-18.03	100.00	100.00	9.00
10	65.65	21.58	28.00	13.07	32.22	0.154	0.043	0.154	0.042	0.00	-2.38	-2.38	26.00
11	55.24	15.51	28.34	11.39	34.88	0.169	0.004	0.114	0.000	-48.25	100.00	100.00	7.00
12	51.29	13.21	28.11	9.58	33.89	0.172	0.002	0.107	0.000	-60.75	100.00	100.00	4.00
13	74.17	14.07	28.31	10.22	32.78	0.249	0.051	0.205	0.043	-21.46	-18.60	2.35	26.00
14	84.34	14.67	29.90	8.50	33.00	0.275	0.065	0.259	0.065	-6.18	0.00	5.82	19.00
15	48.22	9.82	29.90	6.90	33.86	0.169	0.013	0.106	0.003	-59.43	-333.33	-171.79	20.00
16	47.38	8.23	28.31	7.26	33.33	0.172	0.004	0.109	0.000	-57.90	100.00	100.00	8.00
17	65.00	8.69	28.15	4.68	36.76	0.059	0.003	0.049	0.004	-20.41	25.00	37.71	19.00
18	53.93	6.33	27.30	5.70	34.23	0.100	0.003	0.078	0.003	-28.21	0.00	22.00	13.00
19	85.61	16.38	28.00	4.98	36.73	0.067	0.007	0.059	0.010	-13.56	30.00	38.36	21.00
20	85.71	21.27	28.02	3.31	36.59	0.060	0.010	0.055	0.013	-9.09	23.08	29.49	28.00
21	75.33	21.93	28.06	4.50	36.72	0.049	0.006	0.043	0.007	-13.95	14.29	24.78	23.00
22	86.10	28.13	28.28	3.18	35.13	0.048	0.013	0.046	0.014	-4.35	7.14	11.01	26.00
23	75.81	28.11	31.70	6.15	36.93	0.035	0.014	0.033	0.015	-6.06	6.67	12.00	31.00
24	75.10	18.59	31.80	5.92	34.64	0.055	0.017	0.048	0.017	-14.58	0.00	12.73	17.00

In Fig. 3, the influence of the inlet parameters, including pressure and temperature, on the model accuracy is presented. The points listed in Tab. 2 are presented in the carbon dioxide *p-h* diagram. In addition, the motive nozzle mass flow rate error is given at each point. Comparing Figs. 2 and 3 reveal that the investigated range of the motive nozzle operating regimes is wider than in the previous studies. Moreover, Fig. 3 shows the HEM accuracy change within the various parameters. The investigated operating regimes, similar to that investigated by Lucas et al. (2014), result in similar errors, i.e., point #6 or #22.

The operating regimes distributed close to the saturation line (i.e., points #8, #9, #11 and #12) result in decreased HEM accuracy. The decreased accuracy becomes more clear when points #5, #7 and #8 are compared. The errors rapidly increase with decreasing pressure, bringing operating regime close to the saturation line.

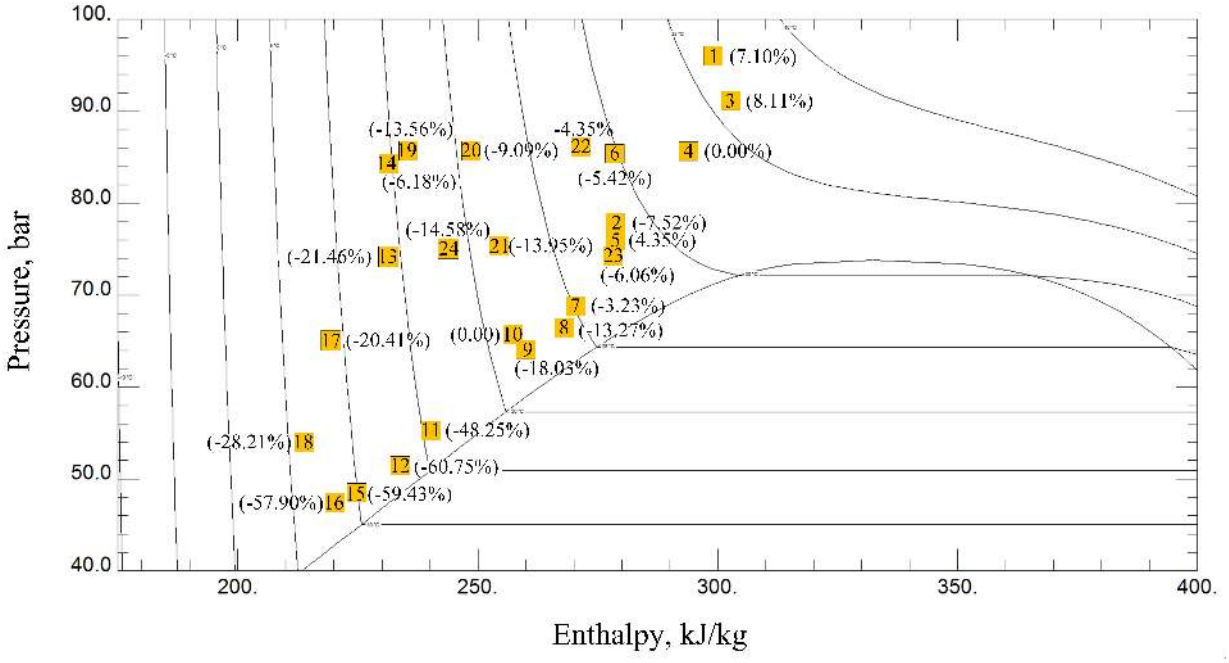

Figure 3: Distribution of the motive nozzle inlet parameters and the corresponding motive nozzle mass flow rate discrepancies in the pressure-enthalpy diagram.

Moreover, the influence of temperature can be observed. Analysing the errors of points #2, #5, #21, #13 and #24 show that the accuracy decreases with decreasing temperature. The same trend can be observed for the group of operating regimes corresponding to the higher motive nozzle inlet pressures (see points #4, #6, #14, #19, #20 and #22).

The results also showed that the expansion inside the diverging part of the motive nozzle proceeds differently for the cases with significant prediction errors. Under the operating conditions for which the mass flow rate relative difference was within 5%, the pressure drop along the motive nozzle was always approximately 40 bars, whereas the pressure drop was substantially smaller for the operating regimes for which the motive nozzle mass flow rate errors were larger. The underestimated pressure drop is one possible reason for the underestimated secondary mass flow rate, and hence the incorrect assessment of χ (e.g., #11 or #12).

4. Conclusions

An analysis of the accuracy of the HEM approach for simulating CO_2 flow inside two-phase transonic ejectors was presented in this study. The investigated range of ejector operating regimes allowed for the accuracy assessment of the HEM approach for simulating of the ejector motive nozzles installed in novel refrigeration units. The results

showed that there is a range of the operating conditions for which HEM provides very accurate results. However, the accuracy of the model strongly depends on the motive nozzle inlet parameters.

In general, we considered relative differences in the motive nozzle mass flow rate of less than 10% as acceptable. Hence, for such a condition, the HEM fidelity is satisfactory. The operating conditions close to or above the critical points can be considered to provide accurate results based on HEM, i.e., both the motive and suction flows are well predicted.

The accuracy of the model decreases with decreasing temperature and pressure. Another important consideration is the decreasing distance to the CO_2 saturation line. The differences between the computed and measured motive nozzle mass flow rates for the operating points distributed near the R744 critical point were the smallest. The errors of these points were comparable to those reported in the literature. That may be caused by high non-equilibrium expansion process for the points far left from the critical point, see Benintendi (2014) and Angielczyk (2010). For such conditions, the HEM assumption that there is thermodynamic and mechanical equilibrium between the vapour and liquid phase is incorrect. Moreover, the density changes in two-phase zone, far left from the critical point, are much more rapid than for the conditions close to the critical point. That may cause additional error in density prediction, hence the mass flow rate prediction. In addition, the results showed that for the accurate solutions, i.e., motive nozzle mass flow errors less than 10%, the flow variables such as pressure, Mach number and velocity are correctly predicted. Nevertheless, the pressure and velocity profiles inside the device should be experimentally investigated to compare experimental results with the computed data.

The presented pressure-enthalpy diagram can be used as a guideline for future CFD-based ejector investigations. The range of the inlet parameters for the accurate results presented here can be used to investigate ejector performances for design and off-design conditions. Moreover, the overall ejector efficiency evaluation based on the model results depends only on χ, as the inlet and outlet pressures are fixed in the numerical approach reported here. Hence, a proper assessment of the mass flow rates is crucial. Furthermore, the results showed that, in some cases, a relatively large difference between the measured and computed primary mass flow rates does not always correspond to a high χ error.

In addition, the HEM approach does not guarantee satisfactory accuracy for low inlet temperatures at the motive nozzle. Similarly, the prediction error increases with decreasing pressure. This accuracy also affected by the proximity to the saturation line. For such conditions, a more complex model should be applied to provide reasonable results.

This conclusion indicates the need for the further work to investigate the accuracy of more complex modelling approaches, such as HRM, or to develop a heterogeneous model for the numerical analysis of R744 ejectors for refrigeration systems.

Acknowledgements

The authors gratefully acknowledge financial support from the Polish Norwegian Research Fund through project No. Pol-Nor/196445/29/2013.

References

Angielczyk, W., 2010. 1-D Modeling Of Supersonic Carbon Dioxide Two-Phase Flow Through Ejector Motive Nozzle. International Refrigeration and Air Conditioning Conference, Purdue.

Attou, A., Seynhaeve, J., 1999. Steady-state critical two-phase flashing flow with possible multiple choking phenomenon: Part 1: Physical modelling and numerical procedure. J. Loss. Prevent. Proc. 12 (5), 335 – 345.

Banasiak, K., Hafner, A., 2011. 1D computational model of a two-phase R744 ejector for expansion work recovery. Int. J. Therm. Sci. 50 (11), 2235 – 2247.

Banasiak, K., Hafner, A., Andresen, T., 2012. Experimental and numerical investigation of the influence of the two-phase ejector geometry on the performance of the R744 heat pump. Int. J. Refrigeration 35 (6), 1617 – 1625.

Banasiak, K., Hafner, A., Kriezi, E. E., Madsen, K. B., Birkelund, M., Fredslund, K., Olsson, R., 2015. Development and performance mapping of a multi-ejector expansion work recovery pack for R744 vapour compression units. Int. J. Refrigeration.

Benintendi, R., 2014. Non-equilibrium phenomena in carbon dioxide expansion. Process Saf. Environ. Prot. 92 (1), 47 – 59, safety Issues for Carbon Capture and Storage.

Chung, T. J., 2010. Computational Fluid Dynamics, 2nd Edition. Cambridge University Press.

Colarossi, M., Trask, N., Schmidt, D. P., Bergander, M. J., 2012. Multidimensional modeling of condensing two-phase ejector flow. Int. J. Refrigeration 35 (2), 290 – 299.

Elbel, S., 2011. Historical and present developments of ejector refrigeration systems with emphasis on transcritical carbon dioxide air-conditioning applications. Int. J. Refrigeration 34 (7), 1545 – 1561.

Elbel, S., Hrnjak, P., 2008. Experimental validation of a prototype ejector designed to reduce throttling losses encountered in transcritical r744 system operation. Int. J. Refrigeration 31 (3), 411 – 422.

Hafner, A., Försterling, S., Banasiak, K., 2014. Multi-ejector concept for R-744 supermarket refrigeration. Int. J. Refrigeration 43, 1–13.

Katto, Y., dec 1969. Dynamics of compressible saturated two-phase flow : Critical flow-sequel, and flow in a pipe. Bulletin of JSME 12 (54), 1417–1427.

Kolev, N. I., 2005. Multiphase flow dynamics 2. Springer.

Lemmon, E. W., Huber, M. L., McLinden, M. O., 2010. NIST Standard Reference Database 23: Reference Fluid Thermodynamic and Transport Properties - REFPROP. National Institute of Standards and Technology, Standard Reference Data Program, Gaithersburg, 9th Edition.

Liu, F., Groll, E. A., 2008. Analysis of a two phase flow ejector for transcritical CO_2 cycle. International Refrigeration and Air Conditioning Conference, Purdue.

Liu, F., Li, Y., Groll, E. A., 2012. Performance enhancement of CO_2 air conditioner with a controllable ejector. Int. J. Refrigeration 35 (6), 1604 – 1616.

Lucas, C., Rusche, H., Schroeder, A., Koehler, J., 2014. Numerical investigation of a two-phase CO2 ejector. Int. J. Refrigeration 43 (0), 154 – 166.

Nakagawa, M., Marasigan, A., Matsukawa, T., Kurashina, A., 2011. Experimental investigation on the effect of mixing length on the performance of two-phase ejector for CO_2 refrigeration cycle with and without heat exchanger. Int. J. Refrigeration 34 (7), 1604 – 1613.

Rusly, E., Aye, L., Charters, W., Ooi, A., 2005. CFD analysis of ejector in a combined ejector cooling system. Int. J. Refrigeration 28 (7), 1092 – 1101.

Smolka, J., Bulinski, Z., Fic, A., Nowak, A. J., Banasiak, K., Hafner, A., Feb. 2013. A computational model of a transcritical R744 ejector based on a homogeneous real fluid approach. Appl. Math. Model. 37 (3), 1208–1224.

Varga, S., Oliveira, A. C., Diaconu, B., 2009. Numerical assessment of steam ejector efficiencies using CFD. Int. J. Refrigeration 32 (6), 1203 – 1211.

Yazdani, M., Alahyari, A. A., Radcliff, T. D., 2012. Numerical modeling of two-phase supersonic ejectors for work-recovery applications. Int. J. Heat Mass Tran. 55 (21-22), 5744–5753.